Proceedings of Montreal 2018
Global Power and Propulsion Forum
7th– 9th May, 2018
www.pps.global

GPPS-2018-0124

INVESTIGATION OF THE EFFECT OF WAVE REFLECTION IN THE FORCED RESPONSE STUDY OF A COMPRESSOR

Zhiping Mao
Department of Mechanical Engineering and Materials Science, Duke University
Durham, United States

Shreyas Hegde
Department of Mechanical Engineering and Materials Science, Duke University
Durham, United States

Tianyu Pan
Department of Mechanical Engineering and Materials Science, Duke University
Durham, United States
School of Energy and Power Engineering, Beihang University
Beijing, China

Robert E. Kielb
Department of Mechanical Engineering and Materials Science, Duke University
Durham, United States

Laith Zori
ANSYS Inc
Lebanon, NH, USA

Rubens Campregher
Ansys Canada Ltd.
Waterloo, ON, Canada

ABSTRACT

The forced response behavior of a rotor in a 3.5-stage compressor rig is studied in this paper. Previous study indicates that the unsteady wave reflection level can highly influence forced response prediction results. Though traditional non-reflecting boundary conditions or mesh treatments can reduce the reflecting waves in the calculation efficiently, in physics the waves will reflect when interacting with the up- and downstream unstimulated bladed rows and non-reflecting is still an approximation. The downstream reflection was identified to have significant influence on the unsteady pressure of the simulated domains. Thus, the aim of this paper is to investigate the potential reflection effect and the consequent influence of forced response due to bladed rows. As an extension of our 3-row stator-rotor-stator (S1-R2-S2) forced response simulation, a 4-row (S1-R2-S2-R3) simulation is conducted to test the influence of 1T-44EO wave reflected from R3 back to R2 domain. Difference is seen compared with the case without the R3 domain, and a destructive interference is observed on forced response behaviors. Two conclusions are drawn from this study: 1) Wave excitation created by downstream stators can reflect upstream due to the existence of the rotor row further downstream. The excitation interacts with the two traditional excitation sources, wake and potential field. In this case, the interaction is destructive and leads to a lower modal force prediction. 2) This reflection from down-stream row has a significant influence on the prediction of forced response, whereas upstream reflection is not significant.3) The cut-on nature of the wave in this case also contributes to the reflection, as the wave propagates without deterioration.

This research also provides a guidance of forced response multi-row modeling.

Keywords: compressor, forced response, wave reflections, multi-excitations

NOMENCLATURE

n	Integer number
s	Pitch
k	Reduced frequency
c	Chord
M	Mach number
u	Velocity
N_b	Number of blades
β	Inter-blade phase angles of excitation
γ	Stagger angles

Acronyms

AR	Acoustic Resonance
IBPA	Inter blade phase angle
IGV	Inlet guide vanes
LE	Leading edge
NSMS	Non-intrusive stress measurement system
ND	Nodal diameter
PS	Pressure side
R1	Rotor 1
R2	Rotor 2
R3	Rotor 3
S1	Stator 1
S2	Stator 2
SS	Suction side
TE	Trailing edge
TT	Time transformation
V	Velocity

1. INTRODUCTION

Vibration, noise and high cycle fatigue failure in turbomachinery are known to be attributed to two major factors i.e. the flutter and forced response. Flutter is caused by the vibration of a blade cascade which in turn leads to aerodynamic forces and it can occur even in a steady flow field (Srinivasan, 1997). This causes energy to be added during each cycle of vibration. It occurs mainly when the damping isn't enough to control the magnitude of aerodynamic forces and this can lead to failure. On the other hand, the major cause for the forced response phenomena is the wake unsteadiness due to the wake effects from the upstream rows. Distortions in the flow can also contribute to forced response along with potential effect from downstream rows. The blade response rises to a maximum value at resonance condition and this occurs at the integral multiples of EO frequencies.

Accurate prediction of forced response requires comprehensive understanding of forcing functions, or external excitations. In turbomachines, the external excitations can be mechanical, thermal or aerodynamic. Since the aerodynamic excitation is the most prevalent it has received the maximum attention in literature. The major causes of aerodynamic excitations are blade-row interactions due to viscous and potential effects, shocks, inlet distortions etc. To model the forced response of a compressor an unsteady simulation is needed to determine its forcing function. This can be done either using a frequency domain method or a time domain method. The former is referred to as the harmonic balance method and is discussed in (Schoenenborn, 2017). The authors carried out the analysis of a multi-row passage compressor configuration. The wake, potential effects from a downstream airfoil which act as disturbances and influence the forced response behavior was discussed. Harmonic balance codes were used for unsteady analysis and the effect of spinning modes was found to influence the circumferentially different blade excitations. The author concluded that the harmonic balance method could be used to predict the circumferential variation for unsteady calculations at a low computational cost. It was also noted that for downstream wakes higher harmonics had to be considered to get a good circumferential distribution whereas a single harmonic was good enough to get the distribution for the upstream wakes. Comparison of the frequency domain method with the time domain method was made by (Vilmin, 2009). It was found that this method gave a significant improvement over the conventional mixing plane technique in time averaged flow estimations of unsteady flow across the rotor interface. The importance of the clocking effects and its relation to the blade number ratio was highlighted in this paper. This turned out to be cost effective computationally and the authors suggested that this method could be used to simulate the inter-blade-row interactions and compare them against results obtained using mixing plane technique. Since this method didn't yield accurate results for the prediction of the forcing function especially for multi-rows multiple passages configurations the time domain method was used in this current paper to overcome the drawback.

The forced response analysis of a 3-row compressor configuration using the time domain method was discussed by Besem (2015) at the crossings indicated in Figure 1. Li (2017) carried out the analysis of the individual and combined effects of the upstream and downstream rows. The maximum response obtained in the simulations was found to be overestimated as compared to experimental results and this was attributed to the downstream wave generated by the Stator 2. To improve the accuracy of the results and overcome the drawbacks of (Besem, 2016), (Li, 2017) the authors quantitatively studied the influence of reflecting boundary condition on the blade modal force and discussed about possible solutions to prevent response behavior from being contaminated by wave reflection. In this regard the authors extended and inflated the inlet and outlet meshes to avoid multiple reflections at the walls and determined the blade pressures and modal forces with the new set of meshes and compared it with the previous results. Additionally, a 5-row simulation was carried out to take an extra source of excitation force, the IGV row with the same blade counts as the other stators, into consideration. Three conclusions were drawn from this study: 1) boundary reflection has a significant

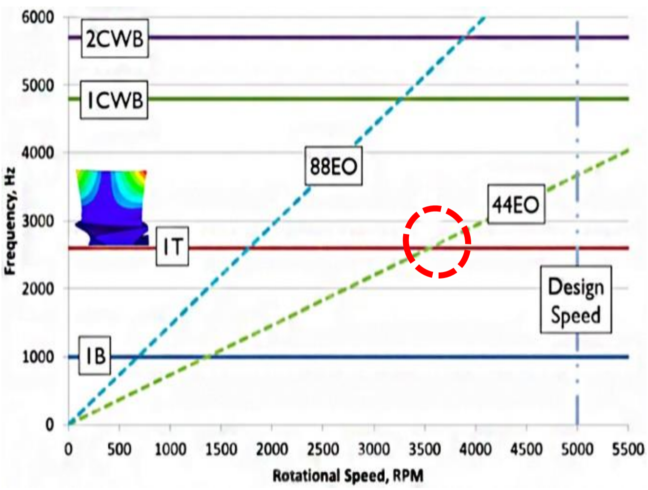

Figure 1 : Campbell Diagram of Purdue configurations. The 1st torsion mode shape of R2 blade is plotted.

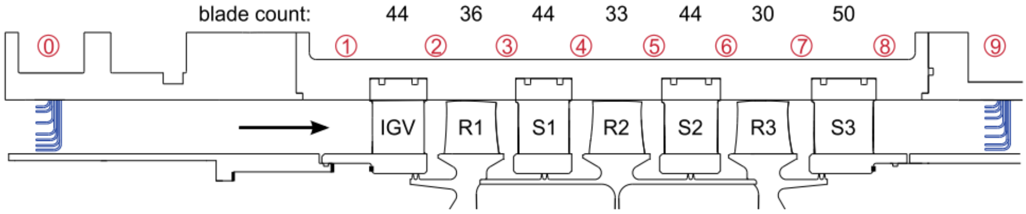

Figure 2 : Purdue 3.5-stage compressor rig. Rotor 2 is mounted with NSMS tip timing and aerodynamic probes.

influence on unsteady simulation and the modal force, thus should be avoided by using mesh treatment up and down stream;2) the IGV wake mildly contributes to the forcing function and cannot be ignored in modeling; 3) the clocking feature of IGV S1 and S2 renders the excitation energy transferred from 1st harmonic to other higher harmonics. This technique used a mesh, the cell size in which was of the order of the wavelength of the unsteady wave and this ensured that the wave was not resolved. Though the forcing function is lowered by using the extension technique, the modal force is still over predicted.

Some authors explored the option of using properties of waves to explain wave propagation and its aeromechanical impact. (Owczarek, 1984) and (Owczarek, 2010) discussed about the phenomena of acoustic resonance in compressors due to wave reflection between an embedded rotor and the upstream and downstream stators. The author provided a methodology to explain the forced vibration in compressors by considering the forced vibration due to reflecting waves by deriving equations based on general wave theory and the airfoil shape of the blades to discuss these phenomena. Since the analysis in the current paper has been done by modeling the 3-D blades, the airfoil shape of the blades has been considered to explain the wave reflection phenomena. The reason for non-synchronized vibration frequencies in test results were attributed to this phenomenon of wave reflection between stages. Three kinds of wave reflections were discussed forward running, backward running and those at a fixed circumferential location in the annulus. The author also discussed about the effects of pressure pulses which could lead to flow separation due to adverse pressure gradient which could in turn lead to a loss in efficiency and initiate stall. However, the aspect of wave reflection between the downstream row and the far field boundary was not discussed and is the focus of the current paper. This wave reflection between the downstream row and the outlet can lead to an acoustic resonance phenomenon the aspect of which is usually neglected by authors. The aero damping can be significantly modified over a small range of inter-blade phase angles by this concept of acoustic resonance and hence it becomes important to predict the same. The formulation to determine the IBPA for a 2-dimensional subsonic flow by Kielb (1983) helps determine the possible angles at which acoustic resonance can occur and further by the theory put forward by Joshua (2017) the wave can be predicted to either propagate without decay (cut-on) or propagate with significant decay (cut-off). Since the current case was 3D a slice of the rotor at mid span was considered for calculations as explained in the later sections of the paper.

2. THREE-ROW CASE ANALYSIS

Although improvement of modal force prediction was obtained with domain extension which helped remove the wave reflection, the remaining discrepancy between the experimental and simulation results motivated further research. There was one main source of inaccuracy in the previous study: only three rows were modeled in the simulation. However, physically there are other bladed rows in the machine, and those rows serves as walls with partial admission to waves. The impact due to the existence of additional rows needs to be studied.

Three row results and discussion

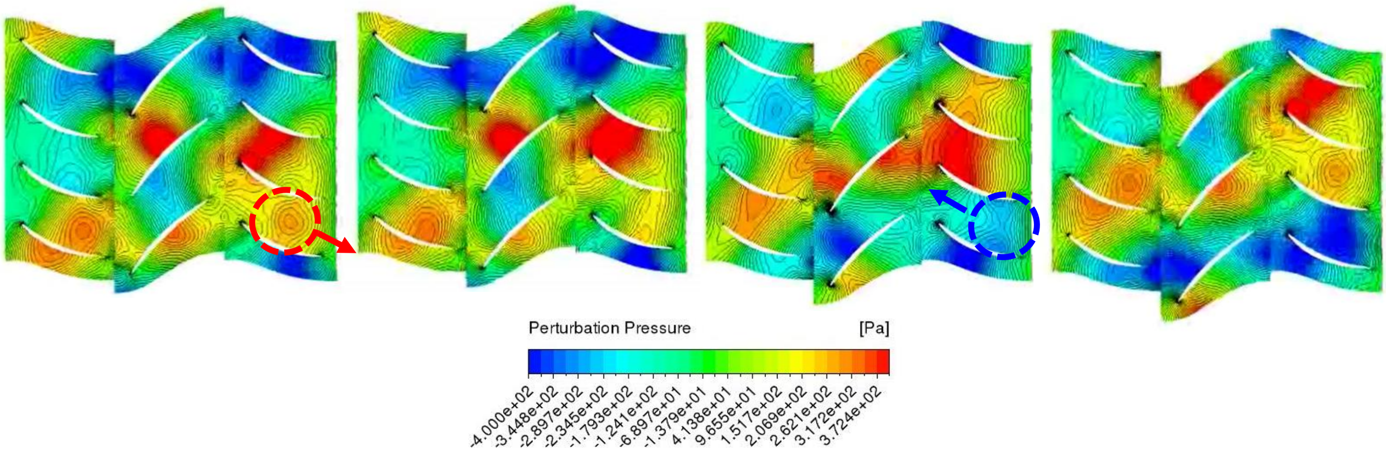

Figure 3 : Perturbation pressure sequence of short domain simulation. The wave marked in red is moving downstream and the one in blue is moving upstream. The sign of the pressure values confirms the same.

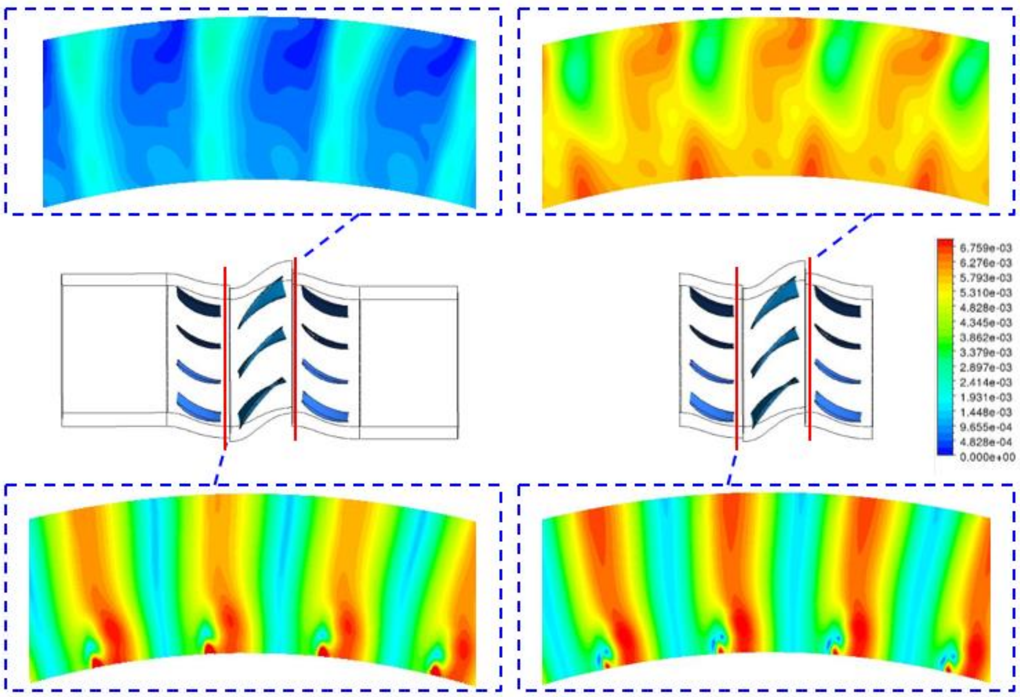

Figure 5 : Contours of unsteady pressure amplitude normalized by reference pressure at different cross sections with location marked on the sketches. Extended three-row simulation is on the left and the original short domain case on the right.

To visualize the propagation of wave reflection, the perturbation pressure is plotted in time sequence. Figure 3 shows the sequential development of pressure perturbation in the 3-row simulation. In this short domain case, reflecting boundary is assigned to the boundary at inlet and exit, same as the setup of Li et al (2015). A positive pressure perturbation volume marked in red travels downstream and attenuates when approaching the downstream boundary. Then a negative pressure volume starts to travel upstream from the boundary. It is further concluded in our prediction that using the inflated mesh can reduce the reflection to a negligible level. A sample of inflated mesh is shown in Figure 5.

To determine the major contributor of wave reflections in our new study, the unsteady pressure amplitude contours are plotted in Figure 4. The extended case with mesh treatment is on the left and the original case on the right. Though both stators have 44 blades and excite the rotor with 44EO components, the strength of waves are different. As observed in the comparison of the original and extended cases, the unsteady level does not differ much at the S1 exit. This indicated that originally there was a limited wave reflection going upstream and reflecting. However, a substantial difference was observed in S2. With the inflated mesh, the unsteady level is much lower compared with the baseline case. The analysis suggests the wave reflection from downstream reflecting boundary condition is the key contributor to the difference between experimental result and our prediction. Accordingly, in our simulation with additional rows, the downstream row, R3, was included.

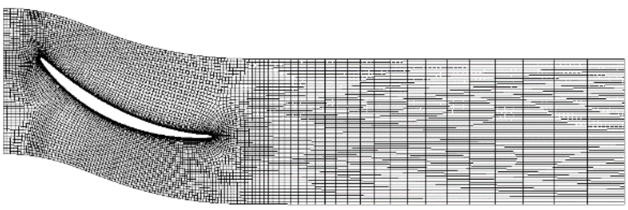

Figure 4 : A sample of S2 mesh treatment used to reduce the wave reflection.

3. FOUR ROW CASE ANALYSIS

Four-row case setup

Figure 6 shows the computational domain of the 4-row case setup, from S1 to R3. In accordance with the test rig the inlet section of the computational domain was extended as the computation also simulated the inlet section of the test rig, starting from station 3 (shown in Figure 2). The mesh was prepared using ANSYS Turbogrid and the subsequent analysis was done using ANSYS CFX. The mesh size consisted of approximately 640000 cells/passage for the extended rows and 540000 for the original case. The SST turbulence model was used. Since the number of wakes shed by an airfoil is the same as the number of airfoils, the entire annulus can be modeled with a few passages and rotational periodicity can be used to capture the entire effect.

The time transformation model is used at the stator-rotor interfaces in the current problem to account for the pitch-change between the rows. The Time-Transformation pitch-change method is based on the time-incline technique of (Giles, 1988) and has been incorporated into ANSYS CFX (ANSYS manual). The time transformation method allows for capturing the correct blade passing frequency if the pitch-ratio between the interfaces are small and not unity. This method was previously validated on compressors with a range of small

Table 1: Comparison of resulting modal force across different cases.

Case label	Case explanation	Commutated modal force, normalized by experimental data	Difference in mass flow, % of experimental data
	Experiment	1	0
a	3-row, no extension	1.64	+0.26%
b	3-row, extended domain, inflated mesh	1.11	+0.13%
c	4-row, extended domain, inflated mesh	0.79	-0.1%

pitch-ratio machines (Qizar et al, 2013), (Zori et al, 2015). Since the method maintain implicit discretization fast solution to a steady periodic state can be achieved efficiently.

The time transformation method provides an added advantage i.e. it conserves the frequency content across the interfaces and this enables the 44EO harmonics content to be visible even in the downstream R3 row. This method was found to be accurate for cases with a different pitch ratio (current case) and therefore was preferred over other methods. The time transformation method uses a blending procedure which helps preserve disturbances across the interfaces. This method being fully implicit, and conservative helps preserve the wake through the interfaces without any disturbance.

The ratio of the number of passages in each row is optimized to achieve sector ratio close to unity. Thus 4, 3, 4, 3 passages are utilized in the S1, R2, S2, R3 domains respectively. Since S1, R2 and S2 blades have 44, 33 and 44 blades respectively with a common factor of 11, the selected 4, 3, 4 is an accurate simplification. As for R3, 3 passages were selected to have the optimized sector ratio with the value closest to 1. Notice that the sector ratio for the S1-R2 and R2-S2 are exactly 1, whereas for S2-R3 the ratio is 1.1. Effectively only the last one interface is using TT model. The R3 mesh was extended as explained earlier by 1.5 times of the original section to reduce the wall reflection which was one of the primary reasons for less accurate results from previous literature. The S1 mesh was also inflated to help capture the wake effects from the upstream rows.

Blade loading aerodynamics

Figure 8 shows the time averaged blade loading for the three and four row cases. As observed the difference in the blade pressures isn't significant in both the cases indicating that the blade loading is preserved even after the addition of an extra rotor.

Modal force analysis

The resulting modal force is shown in Table 1, with the first row representing experimental data and the following three representing simulation data. The experimental modal force was identified by Hall (2017) using the system identification method, and the original data was obtained by using the NSMS system. The experiments were conducted for both the acceleration and deceleration frequency sweep, and the average data was used.

It is noticed that, benchmarking with the experimental data, all simulations over predict the modal force. Comparing cases, a) and b), we observed only a 7% difference. This suggested a limited wave damping effect from the numerical

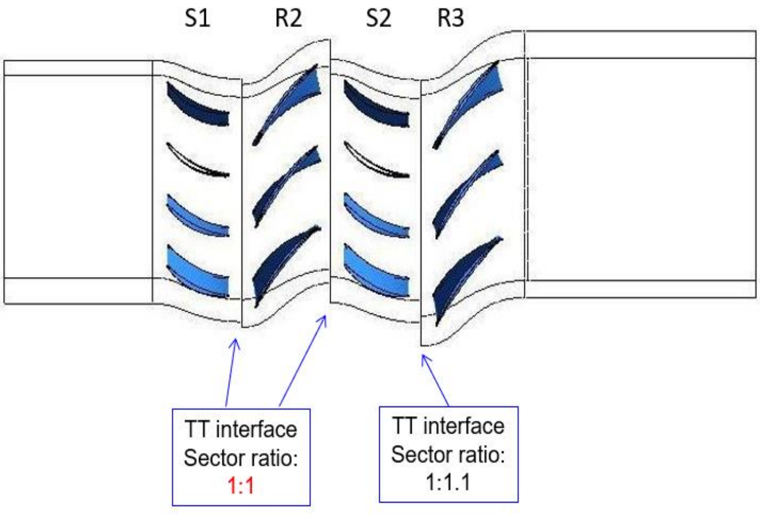

Figure 6 : Sketch of the 4-row simulations. Sector ratios between different rows are marked in two boxes.

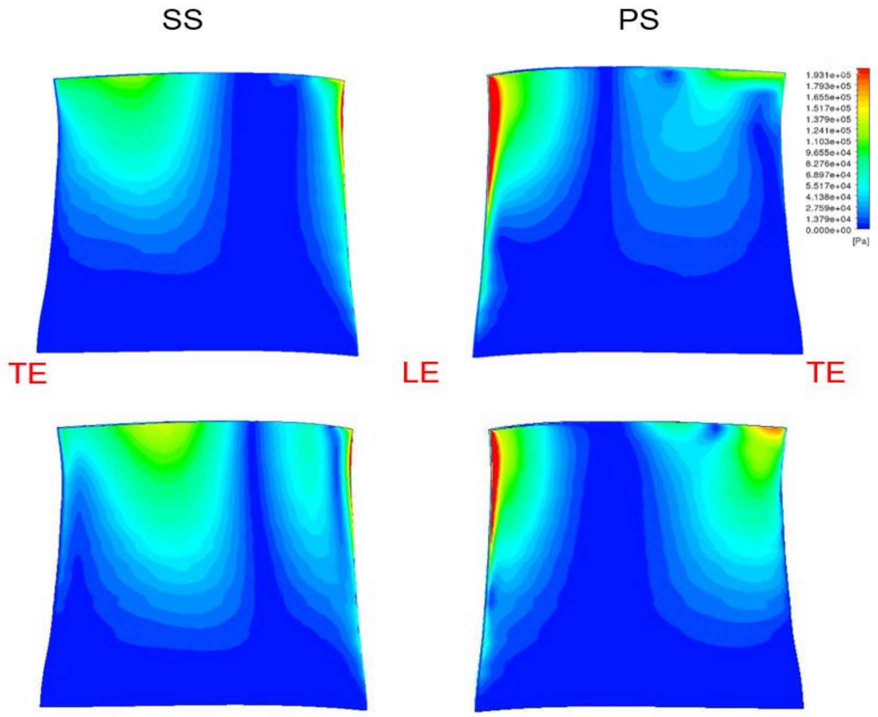

Figure 7 : Modal force distribution on R2 blades. Three-row simulation is on the top and the 4-row case on the bottom.

viscous effect. However, comparing case a) and c), we observed a significant drop in the modal force. It indicated that there was an ineligible wave reflection due to the presence of R3.

To have a closer view of the modal force, the modal force density on R2 is plotted in Figure 7, with the extended 3-row case b) on the top and the extended 4-row case c) at the bottom. It was observed that the magnitude of the modal force on both sides of the blade increases, especially on the pressure side around the trailing edge tip corner and on the suction side along the leading edge. However, though the value in some regions increases, the reflection has a destructive impact on modal force thus the resulting value is lower. This destructive impact is different from the 3-row case, in which the spurious

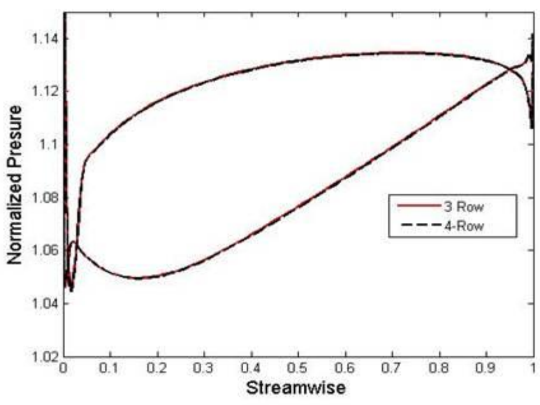

Figure 8 : R2 time-averaged blade loading comparison across different extended domain cases.

reflection has a constructive interference with the original wake and potential field.

The comparison across the cases provides an overview of the impact of wave reflection on forced response behavior. However, the contribution of upstream reflection and downstream reflection is not well presented. To have a deeper understanding, we probed into the two stator stages. The unsteady pressure at the S1 exit and S2 inlet cross-section is shown in Figure 9. As is observed in the comparison of the 3-row and 4-row cases, the unsteady level does not differ much at the S1 exit. This indicates that originally there is limited wave reflection going upstream and reflecting. However, a substantial difference was observed in S2 inlet. When R3 is simulated, the unsteady level is higher compared with the 3-row case without reflection. The analysis suggests the wave reflection from downstream row cannot be ignored, and the blade row does serve as a partial admitted reflecting wall.

Unsteady wave propagation analysis

Figure 10 shows the propagation of unsteady waves in the 4-row configuration. The reflecting wave from R3 passes through S2 and impinges on the SS of R2. This is also justified by the fact that the modal force on the rear part of R2 blades is higher than the 3-row case. As a side note, different from the case in Figure 3, the wave is not reflecting on the boundary as the mesh treatment serves as a wave filter.

Acoustic Resonance Analysis

For two-dimensional subsonic flow, the equation that determines whether an acoustic (pressure) disturbance decays or propagates is given by Kielb et al (1983):

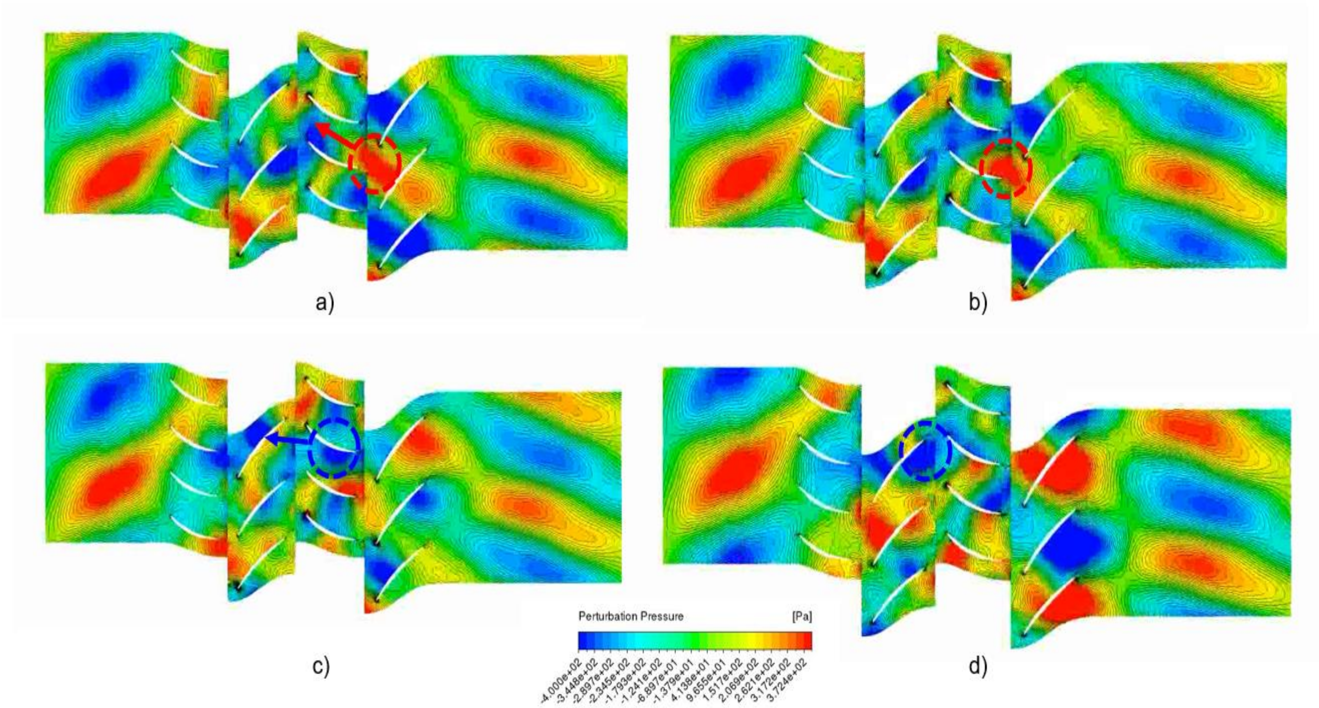

Figure 9 : Perturbation pressure sequence of the 4-row simulation. The wave marked in red is moving reflecting back from R3.

$$\left(\frac{\beta_r + 2\pi n}{s/c}\right)^2 + \frac{4M^2}{M^2 - 1}k\left[k + \frac{(\beta_r + 2\pi n)}{s/c}sin\gamma\right] = 0$$

where β_r is the r-th inter-blade phase angle (IBPA) in radians. The bracketed term $(\beta_r + 2\pi n)$ is bounded between $-\pi$ and π by adjusting the integer multiple n. s/c is the inverse of solidity (c/s) where c is the chord length and s the pitch length. γ is the stagger angle. This equation can be evaluated at both the inlet and exit of the flow domain, where M is the Mach number and k the reduced frequency. The reduced frequency k is based on semi-chord, k=$\omega c/2v$, where ω=$2\pi f$ is the disturbance frequency and v the axial flow velocity. Both M and k are evaluated in the relative frame of reference for a rotating domain.

An acoustic disturbance decays exponentially with distance if the left-hand side of equation is greater than zero ("cut-off") and propagates without decay (a wave-type solution) if the left-hand side is less than zero ("cut-on"). When it is identically zero, it is called an acoustic resonance (AR).

Table 3 : Parameters used for IBPA calculation.

Parameters	Value
V Inlet(m/s)	114.7
V Exit(m/s)	82.01
Mach Number-Inlet	0.3447
Mach Number-Exit	0.2477
Chord-c (m)	0.071
Pitch-s (m)	0.052
Stagger Angle (^{0})	46.2
Reduced Frequency-Inlet	5.3173
Reduced Frequency-Outlet	7.3979

Though the case we are studying is a 3-D case, the blade geometry and flow properties do not vary much across different spans, since the prototype of the rig is a high-pressure compressor. Thus the 2-D method explained above is a good tool to use. The method has been used by Besem (2015) and was proved to be effective. For the current simulation based on the inter blade phase angles and the reduced frequency values were calculated at the inlet and exit of the compressor. Table 2 shows the parameters used for the calculation.

The inlet cut-on region was defined as the area between the two inlet IBPA lines and hence for any angle between them the wave was found to be cut-on i.e. propagate without decay. Since the -11ND wave has an IBPA of -120 deg (calculated based on the definition equation below), it clearly lies in between the 2 lines as indicated in Figure 11. This partially explains why the wave reflection propagates throughout the compressor domain without decay, and to prevent this wave from reflecting from the outlet of the domain an inflation technique was used as explained earlier.

Table 2: IBPA at the inlet and outlet of the compressor

Location		Inter Blade Phase Angle
Inlet	A	-96.1
	B	-147.46
Outlet	A	-131.46
	B	-157.43

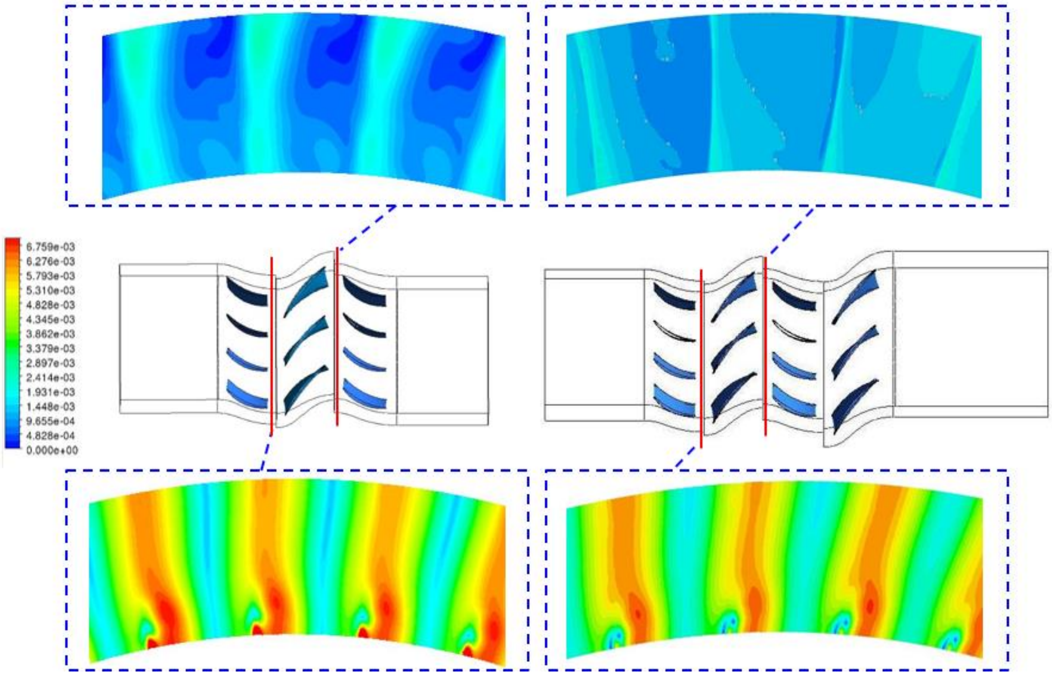

Figure 10 : Normalized unsteady pressure amplitude contours at different cross sections with location marked on the sketches. Extended 3-row simulation is on the left and the 4-row case on the right.

$$ND = \frac{IBPA \cdot N_b}{2\pi}$$

4. CONCLUSIONS AND FUTURE WORK

This paper analyzes a 3.5-stage compressor of an embedded rotor blade (R2) subject to forced response under multiple sources of forcing. We conducted a full 3-D simulation with four rows (S1-R2-S2-R3), as an extension of our 3-row study (S1-R2-S2). The modal force on the embedded R2 was compared across various cases and experimental data, and a significant improvement of prediction accuracy was achieved. Key conclusions are:

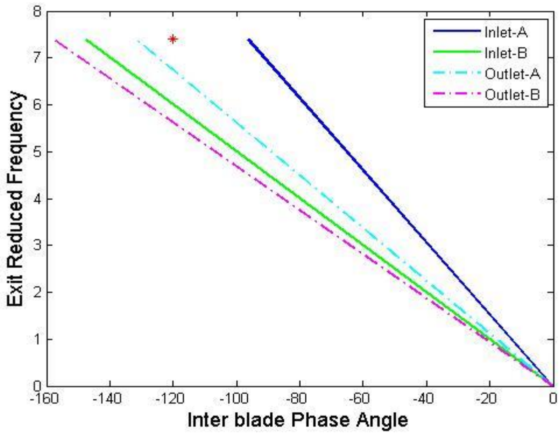

Figure 11 : Acoustic resonance conditions for R2 row. The -11 ND excitation is marked as red star.

1) The reflection from down-stream row has a significant influence on the prediction of forced response, whereas upstream reflection is not significant.

2) Wave excitation created by downstream stators (S2) can reflect upstream due to the existence of the rotor row (R3) further downstream. The excitation interacts with the two traditional excitation sources, wake and potential field. In this case, the interaction is destructive and leads to a lower predicted modal force.

3) The cut-on nature of the wave in this case also contributes to the reflection, as the wave propagates without deterioration.

To extend this research, we consider the following potential topics:

1) Extend the 4-row (S1-R2-S2-R3) case to a 5-row (S1-R2-S2-R3-S3) study. This will help us understand if the wave reflection is fully accounted and to see the reflection level further downstream.

2) Investigate if the wave reflection can be controlled by solidity, axial gap or other design factors and propose a design principle for wave control.

ACKNOWLEDGEMENT

This research is generously sponsored by GUIde Consortium. The authors would like to thank technical support provided by the participating organizations of GUIde 5 Consortium, the experimental results from Zucrow Laboratories at Purdue University.

REFERENCES

[1] Srinivasan, A.V., (1997), Flutter and resonant vibration characteristics of engine blades. Journal of Engineering for Gas Turbines and Power. Transactions of the ASME, vol 119(4), p. 742-775. doi:10.1115/1.2817053.

[2] Schoenenborn, H., (2017), Analysis of the effect of multi-row and multi-passage aerodynamic interaction on the forced response variation in a compressor configuration-Part 1- Aerodynamic excitation. Proceedings of the ASME Turbo Expo: Turbine Technical Conference and Exposition, Volume 7B: Structures and Dynamics. doi:10.1115/GT2017-63018

[3] Gross, J., Krack M., Schoenenborn, H., (2017), Analysis of the effect of multi-row and multi-passage aerodynamic interaction on the forced response variation in a compressor configuration-Part 2- Effect of additional Structural Mistuning. Proceedings of the ASME Turbo Expo: Turbine Technical Conference and Exposition, 2017. Volume 7B: Structures and Dynamics. doi:10.1115/GT2017-63019.

[4] Vilmin S.S., Lorrain E.E., Hirsch C.H., (2009), Application of a Nonlinear Harmonic Method to the Simulation of Clocking Effects. Proceedings of the ASME Turbo Expo: Turbine Technical Conference and Exposition, vol 7 Pt A and B.doi:10.1115/GT2009-59475.

[5] Besem F.M., Kielb R.E., Galpin, P., Zori, L., Key, N.L., (2016), Mistuned Forced Response Predictions of an Embedded Rotor in a Multistage Compressor. Journal of Turbomachinery-Transactions of the ASME. vol 138(6), pp. 106-115. doi:10.1115/1.4032164

[6] Besem F.M., Kielb R.E., Key N.L., (2015), Forced Response Sensitivity of a Mistuned Rotor from an Embedded Compressor Stage. Journal of Turbomachinery-Transactions of the ASME, vol 138(3). Pp, 103-113. doi:10.1115/1.4031866

[7] Li, J., and Kielb. R., (2017), Forcing Superposition and Decomposition of an Embedded Compressor Rotor, Proceedings of the ASME Turbo Expo: Turbine Technical Conference and Exposition, 2017, Vol 7B. doi:10.1115/GT2017-64657

[8] Owczarek J.A., (2011), On the Phenomenon of Pressure Pulses Reflecting Between Adjacent Blade Rows of Turbomachines. ASME Journal of turbomachinery, vol 133, pp 162-171. doi:10.1115/1.4001185

[9] Owczarek J.A., (1984), Analysis of an Axial Compressor Blade Vibration Based on Wave Reflection Theory. ASME. J. Eng. Gas Turbines Power, vol 106(1), pp 57-64. doi:10.1115/1.3239551.

[10] Kielb R. and Kaza, K. (1983), Aeroelastic characteristics of a cascade of mistuned blades in subsonic and supersonic flows, J. Vibration Acoustics., vol 105, pp 425-433. doi:10.1115/1.3269124

[11] Joshua J Waite. (2016), Physical effects, Steady Aerodynamic effects and a design tool for low pressure turbine flutter, Duke University

[12] Hall, K.C., and Hall, S. R., (2016), Private communication

[13] Giles, M., (1988), Calculation of Unsteady Wake/Rotor Interaction. Journal of Propulsion & Power, pp. 356-362

[14] ANSYS CFXR18.0 (2017), Help manual, ANSYS Inc

[15] Qizar, M., Mansour, M., Goswami, S., (2013), Study of Steady State and Transient Blade Row CFD Methods in a Moderately Loaded NASA Transonic High-Speed Axial Compressor Stage. Proceedings of ASME Turbo Expo, 2013/GT2013-94739

[16] Zori, L., Galpin, P., Campregher, R., Morales, J.C., (2015), Time-Transformation Simulation of a 1.5 Stage Transonic Compressor, Journal of Turbomachinery, Vol 139, no. 7, pp. 1139-1152